VERTICAL DIFFERENCING OF FILTERED MODELS

A. Arakawa
Department of Atmospheric Sciences
University of California, Los Angeles, USA

1. INTRODUCTION

In this lecture I shall discuss some of the vertical difference schemes commonly used for the equations that filter inertia-gravity waves through the use of the quasi-geostrophic approximation or a similar but more general approximation.

Most of the numerical weather prediction and general circulation models currently being used are based on the primitive equations. Although a filtering approximation is not explicitly used in such a model (except for the hydrostatic approximation to filter vertically propagating sound waves), its primary objective is still to predict or simulate large-scale disturbances, which are nearly quasi-geostrophic in the extra-tropics. It is therefore instructive to investigate the impact of vertical discretization on such disturbances using filtered models. In this way we should be able to obtain some insight into the behavior of such disturbances in vertically discrete primitive equation models.

2. THE QUASI-GEOSTROPHIC SYSTEM OF EQUATIONS

When pressure p is used as the vertical coordinate, the quasi-geostrophic system of equations under frictionless and adiabatic processes consists of the following equations:

Vorticity equation

$$\left(\frac{\partial}{\partial t} + \mathbf{v}_g \cdot \nabla \right)(\zeta_g + f) + f_o \nabla \cdot \mathbf{v} = 0 \; ; \tag{1}$$

Thermodynamic equation

$$\left(\frac{\partial}{\partial t} + \mathbf{v}_g \cdot \nabla \right) \theta + \omega \frac{d\overline{\theta}}{dp} = 0 \; ; \tag{2}$$

Continuity equation

$$\nabla \cdot \mathbf{v} + \frac{\partial \omega}{\partial p} = 0 \; ; \tag{3}$$

Hydrostatic equation

$$\frac{\partial \phi}{\partial p} = - \alpha \; ; \tag{4}$$

Equation of state

$$\theta \equiv \left(\frac{p_o}{p}\right)^{\kappa} T = \left(\frac{p_o}{p}\right)^{\kappa} \frac{p}{R} \alpha \; . \tag{5}$$

Here $\partial/\partial t$ and ∇ are the time derivative and horizontal gradient operators, respectively, under constant pressure; $\mathbf{v}_g$ is the geostrophic velocity given by

$$\mathbf{v}_g = \mathbf{k}\times\nabla\psi, \quad \psi \equiv \frac{\phi}{f_o} \;; \tag{6}$$

$\mathbf{k}$ is the vertical unit vector; ψ is the geostrophic streamfunction; ϕ is the geopotential gz; g is the acceleration due to gravity; z is height; f_o is a characteristic value of the coriolis parameter f; ζ_g is the geostrophic vorticity given by

$$\zeta_g = \mathbf{k}\cdot\nabla\times\mathbf{v}_g = \nabla^2\psi \;; \tag{7}$$

$\mathbf{v}$ is the (non-geostrophic) horizontal velocity; θ is the potential temperature; ω is the individual time derivative of the pressure, dp/dt; $\overline{\theta}$ is a standard potential temperature, which is a function of p only; α is the specific volume; $\kappa \equiv R/c_p$; R is the gas constant; and c_p is the specific heat at constant pressure. For derivation and justification of these equations, see for example, Holton (1979) or Haltiner and Williams (1980).

Eliminating $\nabla\cdot\mathbf{v}$ between (1) and (3), and using (7), we obtain

$$\left(\frac{\partial}{\partial t} + \mathbf{v}_g\cdot\nabla \right)\left(\nabla^2\psi + f \right) - f_o \frac{\partial\omega}{\partial p} = 0. \tag{8}$$

Multiplying (2) by $-(\alpha/\theta)/f_o$, which is a function of p only, and using (4) and the definition of ψ, we obtain

$$\left(\frac{\partial}{\partial t} + \mathbf{v}_g\cdot\nabla \right) \frac{\partial\psi}{\partial p} + \frac{\omega}{f_o} S = 0 \;, \tag{9}$$

where S is a static stability parameter defined by $S \equiv -(\alpha/\theta)d\overline{\theta}/dp$, which is a function of p only.

We may further eliminate ω between (8) and (9). Then we obtain

$$\left(\frac{\partial}{\partial t} + \mathbf{v}_g\cdot\nabla \right) q = 0, \qquad q \equiv \nabla^2\psi + f + f_o^2 \frac{\partial}{\partial p}\left(\frac{1}{S}\frac{\partial\psi}{\partial p}\right), \tag{10}$$

where q is the <u>quasi-geostrophic</u> <u>(pseudo-)</u> <u>potential</u> <u>vorticity</u>. In deriving (10), we have used $(\partial\mathbf{v}_g/\partial p)\cdot\nabla(\partial\psi/\partial p) = 0$. At the upper ($p = p_T$) and lower ($p = p_S$) boundaries, we assume $\omega = 0$. Then from (9),

$$\left(\frac{\partial}{\partial t} + \mathbf{v}_g\cdot\nabla \right) \frac{\partial\psi}{\partial p} = 0 \quad \text{at } p = p_T,\ p_S \;. \tag{11}$$

Equations corresponding to (10) and (11) but with height z as the vertical coordinate can formally be obtained by reinterpreting $\partial/\partial t$ and ∇ as those under constant z and rewriting $\partial/\partial p$ as $-(1/\overline{\rho}g)\partial/\partial z$. Then (10) becomes

$$\left(\frac{\partial}{\partial t} + \mathbf{v}_g\cdot\nabla \right) q = 0, \qquad q \equiv \nabla^2\psi + f + \frac{f_o^2}{\overline{\rho}} \frac{\partial}{\partial z}\left(\frac{\overline{\rho}}{N^2}\frac{\partial\psi}{\partial z}\right), \tag{12}$$

where $\bar{\rho}$ is a standard density, which is a function of z only, N is the Brunt-Väisälä frequency defined by $N^2 \equiv g\, d\ell n\bar{\theta}/dz$, which is also a function of z only, and the relation $S = (N/\bar{\rho}g)^2$ has been used. Eq. (11) becomes

$$\left(\frac{\partial}{\partial t} + \mathbf{v}_g \cdot \nabla \right) \frac{\partial \psi}{\partial z} = 0 \quad \text{at} \quad z = z_S, z_T \quad , \tag{13}$$

where z_S and z_T are the heights of the lower and upper boundaries, respectively.

3. CONSERVATION LAWS FOR QUASI-GEOSTROPHIC FLOW

Before proceeding to the problem of vertical differencing, let us consider some important integral constraints on quasi-geostrophic flow. For simplicity, we shall use the β-plane approximation, in which the effect of the earth's curvature is neglected except for the meridional gradient of the coriolis parameter f.

We introduce the cartesian coordinates x (directed eastward) and y (directed northward), and let $\beta \equiv df/dy$ be constant. Using the linear differential operator L whose form in the pressure coordinate is given by

$$L(\psi) \equiv \nabla^2\psi + f_o^2 \frac{\partial}{\partial p}\left(\frac{1}{S}\frac{\partial \psi}{\partial p}\right), \tag{14}$$

we may rewrite (10) as

$$\frac{\partial}{\partial t} L(\psi) = J(\, L(\psi),\, \psi\,) - \beta\frac{\partial \psi}{\partial x} , \tag{15}$$

while (11) as

$$\frac{\partial}{\partial t}\frac{\partial \psi}{\partial p} = J\left(\frac{\partial \psi}{\partial p} ,\, \psi \right) \quad \text{at} \quad p = p_T,\, p_S \quad . \tag{16}$$

Here J(a, b) is the Jacobian given by

$$J(a,\, b) \equiv \frac{\partial a}{\partial x}\frac{\partial b}{\partial y} - \frac{\partial a}{\partial y}\frac{\partial b}{\partial x} \quad . \tag{17}$$

From the integral properties of the Jacobian, we obtain from (15)

$$\frac{\partial}{\partial t} \overline{L(\psi)} = 0 \ , \tag{18}$$

$$\frac{\partial}{\partial t} \frac{1}{2} \overline{[L(\psi)]^2} = - \beta\, \overline{\frac{\partial \psi}{\partial x} L(\psi)} \ , \tag{19}$$

$$\overline{\psi \frac{\partial}{\partial t} L(\psi)} = 0 \tag{20}$$

at each pressure level. Here the overbar denotes the horizontal area mean, along an isobaric surface, over a domain that is periodic in x and bounded by vertical walls at two latitudes along which ψ = constant in x. Similarly, from (16),

$$\frac{\partial}{\partial t} \overline{\frac{\partial \psi}{\partial p}} = 0 \quad , \tag{21}$$

$$\frac{\partial}{\partial t} \frac{1}{2} \overline{\left(\frac{\partial \psi}{\partial p}\right)^2} = 0 \quad , \tag{22}$$

$$\overline{\psi \frac{\partial}{\partial t} \frac{\partial \psi}{\partial p}} = 0 \tag{23}$$

at $p = p_S$, p_T. (Since $\bar{\omega} = 0$ for such a domain, (21) is valid at all pressure levels, as can be seen from (9).)

From $\nabla^2\psi = \partial^2\psi/\partial x^2 + \partial^2\psi/\partial y^2$ we find

$$\overline{\frac{\partial \psi}{\partial x} \nabla^2\psi} = \overline{\frac{\partial}{\partial x} \frac{1}{2} \left[\left(\frac{\partial \psi}{\partial x}\right)^2 - \left(\frac{\partial \psi}{\partial y}\right)^2 \right] + \frac{\partial}{\partial y} \left(\frac{\partial \psi}{\partial x} \frac{\partial \psi}{\partial y}\right)} \quad , \tag{24}$$

which vanishes for the domain being considered. Then (19) becomes

$$\frac{\partial}{\partial t} \frac{1}{2} \overline{[L(\psi)]^2} = - \beta f_o^2 \overline{\frac{\partial \psi}{\partial x} \frac{\partial}{\partial p}\left(\frac{1}{S} \frac{\partial \psi}{\partial p}\right)} \quad . \tag{25}$$

Integrating (25) by parts with respect to p from $p = p_T$ to $p = p_S$, we obtain

$$\frac{\partial}{\partial t} \int_{p = p_T}^{p = p_S} \frac{1}{2} \overline{[L(\psi)]^2} \, dp = - \beta f_o^2 \left[\frac{1}{S} \overline{\frac{\partial \psi}{\partial x} \frac{\partial \psi}{\partial p}} \right]_{p_T}^{p_S} \quad , \tag{26}$$

which vanishes if $\partial\psi/\partial p$ is constant at $p = p_S$ and $p = p_T$ (i.e., the lower and upper boundaries are isothermal or isentropic surfaces), as Charney (1971) pointed out.

Similarly, integrating (20) by parts and using (23), we find

$$\frac{\partial}{\partial t} \int_{p = p_T}^{p = p_S} \frac{1}{2} \overline{\left[(\nabla\psi)^2 + \frac{f_o^2}{S} \left(\frac{\partial \psi}{\partial p}\right)^2 \right]} \, dp = 0 \quad . \tag{27}$$

The first term in the integrand is the kinetic energy of the geostrophic wind per unit mass, while from (6) and (4) the second term becomes $\frac{1}{2} \overline{\alpha^2}/S$, which is the available potential energy of the quasi-geostrophic system per unit mass.

Based on the analogy of the conservation laws (26), with the vanishing right hand side, and (27) to enstrophy and energy conservation for two-dimensional incompressible flow, Charney (1971) developed a theory of quasi-geostrophic turbulence.

4. THE CHARNEY-PHILLIPS VERTICAL DIFFERENCING

Charney and Phillips (1953) introduced a vertical differencing of the equations governing quasi-geostrophic flow based on the vertical grid shown by Fig. 1. Here ℓ is the index identifying pressure levels. The geostrophic streamfunction ψ is carried at the integer levels, while ω and θ (or $\partial\psi/\partial p$) are carried at the half-integer levels. Correspondingly, (8) is applied to the integer levels and (9) is applied to the half-integer levels. In this lecture, this vertical grid is refered to as the Charney-Phillips grid, or the CP-grid.

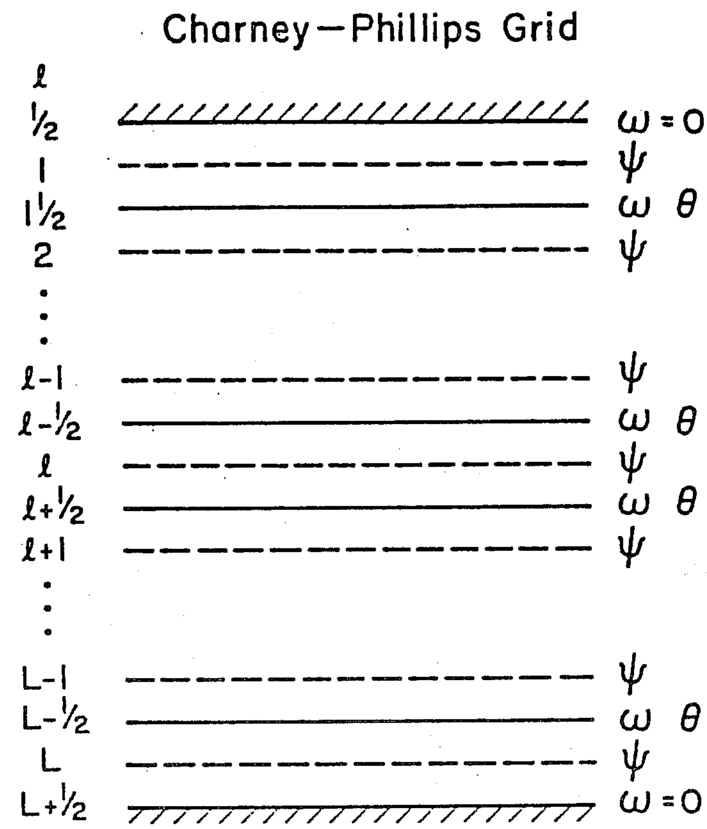

Fig. 1 The vertical grid used by Charney and Phillips (1953). See text for explanations.

By using the most straight-forward vertical differencing of $\partial\omega/\partial p$ and $\partial\psi/\partial p$, we may write the discrete version of (8) and (9) as

$$\frac{\partial}{\partial t}\nabla^2\psi_\ell = -\mathbf{v}_\ell\cdot\nabla(\nabla^2\psi_\ell + f) + f_o\frac{\omega_{\ell+\frac{1}{2}} - \omega_{\ell-\frac{1}{2}}}{(\Delta p)_\ell}$$

for $\ell = 1, 2, \cdots, L$, (28)

$$\frac{\partial}{\partial t}\frac{\psi_{\ell+1} - \psi_\ell}{(\Delta p)_{\ell+\frac{1}{2}}} = -\mathbf{v}_{\ell+\frac{1}{2}}\cdot\nabla\frac{\psi_{\ell+1} - \psi_\ell}{(\Delta p)_{\ell+\frac{1}{2}}} - \frac{S_{\ell+\frac{1}{2}}}{f_o}\omega_{\ell+\frac{1}{2}}$$

for $\ell = 1, 2, \cdots, L-1$, (29)

where

$$(\Delta p)_\ell \equiv p_{\ell+\frac{1}{2}} - p_{\ell-\frac{1}{2}}, \quad (\Delta p)_{\ell+\frac{1}{2}} \equiv p_{\ell+1} - p_\ell , \qquad (30)$$

$$\mathbf{v}_{\ell+\frac{1}{2}} \equiv \frac{1}{2}(\mathbf{v}_\ell + \mathbf{v}_{\ell+1}). \qquad (31)$$

Note that for $\ell = 1$ and $\ell = L$, the boundary conditions $\omega_{\frac{1}{2}} = 0$ and $\omega_{L+\frac{1}{2}} = 0$ can be directly incorporated into (28), so that (29) applied to $\ell = 0$ and $\ell = L$, which corresponds to (11), is not necessary.

Eliminating non-zero ω's for $\ell = 1\frac{1}{2}, 2\frac{1}{2}, \ldots, L-\frac{1}{2}$ between (28) and (29), and using $\mathbf{v}_{\ell+\frac{1}{2}} \cdot \nabla(\psi_{\ell+1} - \psi_\ell) = \mathbf{v}_\ell \cdot \nabla(\psi_{\ell+1} - \psi_\ell) = \mathbf{v}_{\ell+1} \cdot \nabla(\psi_{\ell+1} - \psi_\ell)$, we obtain

$$\frac{\partial}{\partial t} q_\ell = - \mathbf{v}_\ell \cdot \nabla q_\ell \quad , \tag{32}$$

where the subscript g for $\mathbf{v}$ has been omitted, and

$$q_1 = \nabla^2\psi_1 + f + \frac{f_o^2}{(\Delta p)_1} \frac{\psi_2 - \psi_1}{(S\Delta p)_{1\frac{1}{2}}} \, , \tag{33}$$

$$q_\ell = \nabla^2\psi_\ell + f + \frac{f_o^2}{(\Delta p)_\ell} \left[\frac{\psi_{\ell+1} - \psi_\ell}{(S\Delta p)_{\ell+\frac{1}{2}}} - \frac{\psi_\ell - \psi_{\ell-1}}{(S\Delta p)_{\ell-\frac{1}{2}}} \right] \text{ for } \ell=2, 3, \ldots, L-1, \tag{34}$$

$$q_L = \nabla^2\psi_L + f - \frac{f_o^2}{(\Delta p)_L} \frac{\psi_L - \psi_{L-1}}{(S\Delta p)_{L-\frac{1}{2}}} \; . \tag{35}$$

It should be noted that (34) can be derived through a straight-forward differencing of (10), but (33) and (35) cannot. This is because the boundary condition $\omega = 0$ has already been used in the definition of q. In fact, the limit of (35), for example, as $(\Delta p)_L$ and $(\Delta p)_{L-\frac{1}{2}}$ approach zero gives

$$q_S = \nabla^2\psi_S + f - \frac{f_o^2}{p_S - p_S{-}} \left(\frac{1}{S} \frac{\partial\psi}{\partial p} \right)_{p = p_S{-}} \; . \tag{36}$$

Here p_S- is the pressure slightly above the surface. This does not agree with the surface value of q defined by (10); but it does agree with the modified potential vorticity $\tilde{q}$ discussed by Bretherton (1966), which is defined by

$$\tilde{q} \equiv q - \left(\frac{f_o^2}{S} \frac{\partial\psi}{\partial p} \right)_{p = p_S} \delta(p_S - p) + \left(\frac{f_o^2}{S} \frac{\partial\psi}{\partial p} \right)_{p = p_T} \delta(p - p_T) \quad , \tag{37}$$

where δ is the Dirac delta function. (To see the agreement, integrate (37) with respect to p from p_S- to p_S after substitution of q given by (10) and then divide the result by $p_S - p_S-$.) If we modify the operator $L(\psi)$ to $\tilde{L}(\psi)$ following the modification of q to $\tilde{q}$ and if $\tilde{L}(\psi)$ is used in place of $L(\psi)$ in (15), we can show that

$$\frac{\partial}{\partial t} \int_{p_T}^{p = p_S} \overline{\frac{1}{2} \, [\tilde{L}(\psi)]^2} \, dp = 0 \quad . \tag{38}$$

One of the major advantages of the vertical differencing presented here is that the governing equation can be compactly written in the form of (32), which is a discrete analog of

$$\frac{\partial}{\partial t} \tilde{q} \equiv - \mathbf{v}_g \cdot \nabla\tilde{q} \tag{39}$$

for the continuous case. Corresponding to (38), we can show that

$$\frac{\partial}{\partial t}\frac{1}{2}\left[\overline{\{ \nabla^2\psi_1 \ (\Delta p)_1 + f_o^2 \ \frac{\psi_2 - \psi_1}{(S\Delta p)_{1\frac{1}{2}}} \}^2}\right.$$
$$+\sum_{\ell=2}^{L-1} \overline{\{ \nabla^2\psi_\ell \ (\Delta p)_\ell + f_o^2 \left(\frac{\psi_{\ell+1} - \psi_\ell}{(S\Delta p)_{\ell+\frac{1}{2}}} - \frac{\psi_\ell - \psi_{\ell-1}}{(S\Delta p)_{\ell-\frac{1}{2}}} \right) \}^2}$$
$$\left. + \overline{\{ \nabla^2\psi_L \ (\Delta p)_L - f_o^2 \ \frac{\psi_L - \psi_{L-1}}{(S\Delta p)_{L-\frac{1}{2}}} \}^2} \right] = 0 \ . \qquad (40)$$

We can also show that the vertical differencing presented here satisfies

$$\frac{\partial}{\partial t}\left[\sum_{\ell=1}^{L} \overline{\frac{1}{2}\,(\nabla\psi_\ell)^2(\Delta p)_\ell} + \sum_{\ell=1}^{L-1} \overline{\frac{f_o^2}{2}\,\frac{(\psi_{\ell+1} - \psi_\ell)^2}{(S\Delta p)_{\ell+\frac{1}{2}}}}\right] = 0 \ , \qquad (41)$$

which is a discrete analog of (27).

5. TOTAL POTENTIAL ENERGY, AVAILABLE POTENTIAL ENERGY AND GROSS STATIC STABILITY

Before describing Lorenz's approach in vertical differencing, let us briefly review in this section the concepts of total potential energy, available potential energy and gross static stability, as presented by Lorenz (1955, 1960).

Energy of the atmosphere consists of kinetic energy, internal energy, potential energy and the latent energy of water vapor. Here we ignore phase changes of water so that only the first three need to be considered. The kinetic energy of the entire atmosphere is given by

$$K = \int \frac{1}{2}\,\mathbf{v}^2 dM \ , \qquad (42)$$

where dM is an element of mass of the atmosphere. Similarly, the internal and potential energy of the entire atmosphere are given by

$$I = \int c_v T \ dM, \qquad (43)$$

$$P = \int \phi \ dM, \qquad (44)$$

where c_v is the specific heat at constant volume. When the hydrostatic approximation (4) is used, we obtain, through integration by parts,

$$P = \int \frac{1}{g}\int_0^{p_S} \phi dp \ dS$$

$$= \int \frac{1}{g} \left[[\phi p]_{p=0}^{p=p_S} + \int_0^{p_s} p\alpha dp \right] dS$$

$$= \int \frac{1}{g} \phi_S p_S dS + \int RT \; dM \qquad (45)$$

where $\int dS$ is the area integral over the entire globe. Using $R = c_p - c_v$, we obtain

$$P + I = \int \frac{1}{g} \phi_S p_S dS + \int c_p T \; dM. \qquad (46)$$

The sum of P and I is called the <u>total potential energy</u>. If the surface pressure p_S is approximately constant in time and space, as we have been assuming in the previous section, we obtain, approximately,

$$\frac{d}{dt} (P + I) = \int c_p \frac{\partial \overline{T}}{\partial t} dM. \qquad (47)$$

Conservation of the total energy is given by

$$\frac{d}{dt} (P + I + K) = 0. \qquad (48)$$

In the quasi-geostrophic system of equations, however, $\partial(\overline{\partial\psi/\partial p})/\partial t = 0$ at all pressure levels (see the statement in the parentheses below (23)), and, therefore, $\partial\overline{T}/\partial t = 0$ at all pressure levels. Use of (47) in (48) then shows that conservation of the total energy is generally not satisfied with the quasi-geostrophic form of the thermodynamic equation (2).

When $\phi_S = 0$, use of the potential temperature θ in (46) gives

$$P + I = \frac{c_p}{p_o^{\kappa}} \int p^{\kappa} \theta \; dM. \qquad (49)$$

<u>Available potential energy</u> is a portion of the total potential energy which may be available for conversion into kinetic energy, and it is equal to the excess of total potential energy, above the total potential energy which would be present if the atmosphere were to be rearranged, under isentropic changes of state, to possess horizontal isentropic surfaces, with stable stratification. (This isentropic arrangement of mass is illustrated in Fig. 2 by the open arrow.) The resulting value of P + I after the rearrangement would be obtained by replacing p^{κ} in (49) by $\tilde{p}^{\kappa}$, where $\tilde{p}$ is the average value of p on each isentropic surface, which is an invariant under isentropic processes. Thus the available potential energy is given by

$$A = \frac{c_p}{p_o^{\kappa}} \int (p^{\kappa} - \tilde{p}^{\kappa}) \theta \; dM. \qquad (50)$$

From the definition of A, it is clear that dA/dt = d(P + I)/dt, so that

$$\frac{d}{dt} (A + K) = 0. \qquad (51)$$

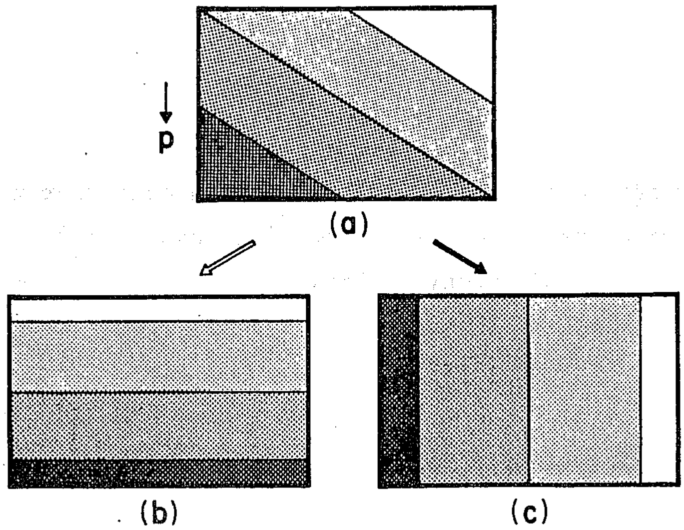

Fig. 2 Vertical cross-sections showing air separated by isentropic (θ = const.) surfaces. (a): Given state. (b) and (c): Hypothetical states that could be obtained from (a) through isentropic rearrangement of mass. The excess of (P + I) for (a) above that for (b) is the available potential energy and the deficit of (P + I) for (a) below that for (c) is the gross static stability.

Analogously, gross static stability is equal to the deficit of total potential energy, below the total potential energy which would be present if the mass of the atmosphere is to be rearranged, under isentropic changes of state, to possess vertical isentropic surfaces. (This isentropic rearrangement of mass is illustrated in Fig. 2 by the solid arrow.) The resulting value of P + I after the rearrangement would be obtained by replacing p^κ in (40) by its average value over the mass of a vertical column, i.e., $p_S^\kappa/(1+\kappa)$. Thus the gross static stability is given by

$$S = \frac{c_p}{p_o^\kappa} \int \left(\frac{p_S^\kappa}{1+\kappa} - p^\kappa \right)\theta \, dM. \qquad (52)$$

(This S must be distinguished from the previously defined $-(\alpha/\theta)d\bar{\theta}/dp$.) Integration by parts yields

$$S = \frac{1}{1+\kappa} \frac{c_p}{p_o^\kappa} \int (p_S^\kappa p - p^{1+\kappa}) \left(- \frac{\partial\theta}{\partial p} \right) dM, \qquad (53)$$

which is a weighted mean of $-\partial\theta/\partial p$. Note that

$$\frac{d}{dt} \int c_p \theta \, dM = 0 \qquad (54)$$

under isentropic processes. Taking into account (54) and (49), we see from (52) that

$$\frac{d}{dt} S = - \frac{d}{dt} (P + I) \ , \tag{55}$$

so that, from (48),

$$\frac{d}{dt} S = \frac{d}{dt} K \ . \tag{56}$$

Thus, the gross static stability increases as kinetic energy increases. This is due to the mean vertical transport of potential enthalpy, $c_p\theta$, associated with the conversion from potential energy to kinetic energy. For a dynamical consequence of this stabilization, see Arakawa (1962).

In the quasi-geostrophic system of equations presented in Section 2, the relation (51) holds in an approximated form, as shown by (27). But it fails to satisfy the relations (48) and (56).

6. THE LORENZ VERTICAL DIFFERENCING FOR THE BALANCED SYSTEM OF EQUATIONS

Lorenz (1960) discussed the energetics of a filtered model in which the balance equation (Charney, 1955) is used as a filtering approximation. The model consists of the following system of equations:

Vorticity equation

$$(\frac{\partial}{\partial t} + \mathbf{v}_\psi \cdot \nabla)(\zeta + f) + \nabla \cdot [(\zeta + f)\mathbf{v}_\chi + \omega \frac{\partial}{\partial p} \nabla \psi] = 0; \tag{57}$$

Balance equation

$$\nabla^2 \phi = \nabla \cdot [(\zeta + f)\nabla\psi - \nabla \frac{1}{2} v_\psi^2]; \tag{58}$$

Thermodynamic equation

$$(\frac{\partial}{\partial t} + \mathbf{v}_\psi \cdot \nabla)\theta + \nabla \cdot (\mathbf{v}_\chi \theta) + \frac{\partial}{\partial p}(\omega\theta) = 0, \tag{59}$$

Continuity equation

$$\nabla \cdot \mathbf{v}_\chi + \frac{\partial}{\partial p}\omega = 0. \tag{60}$$

The hydrostatic equation and the equation of state remain the same as (4) and (5), respectively. We have used the notations

$$\mathbf{v} = \mathbf{v}_\psi + \mathbf{v}_\chi, \qquad \mathbf{v}_\psi = \mathbf{k} \times \nabla\psi \qquad \mathbf{v}_\chi = \nabla\chi, \tag{61}$$

where ψ is the streamfunction, which is generally not the same as that of geostrophic velocity, and χ is the velocity potential. The balance equation (58) is a simplified form of the divergence equation and gives a more general balance between ψ and ϕ than that of pure geostrophy.

It can be shown that the above system of equations satisfies all of the conservation laws presented in Section 5, the only modification being that $\frac{1}{2} v^2$ is replaced by $\frac{1}{2} v_{\psi}^2$. Lorenz (1960) presented a vertically discrete version of this system, following an approach that could best be described by his own statements quoted below.

"Let us now replace the three-dimensional atmosphere by n layers, bounded by the n + 1 isobaric surfaces .... We must now replace the system of differential equations by a modified system in which finite differences replace derivatives with respect to p. Our problem is to do this in such a way that reversible adiabatic processes still have numerically equal effects upon kinetic energy, total potential energy, available potential energy, and gross static stability. To this end, we define θ and ψ within each layer. At this point we depart from many of the currently used models in which the wind field is defined at n levels and the temperature field at n - 1 levels (see Charney and Phillips, 1953)."

Fig. 3 shows the vertical grid on which the Lorenz vertical differencing is based. In this lecture, this vertical grid is referred to as the Lorenz grid, or the L-grid.

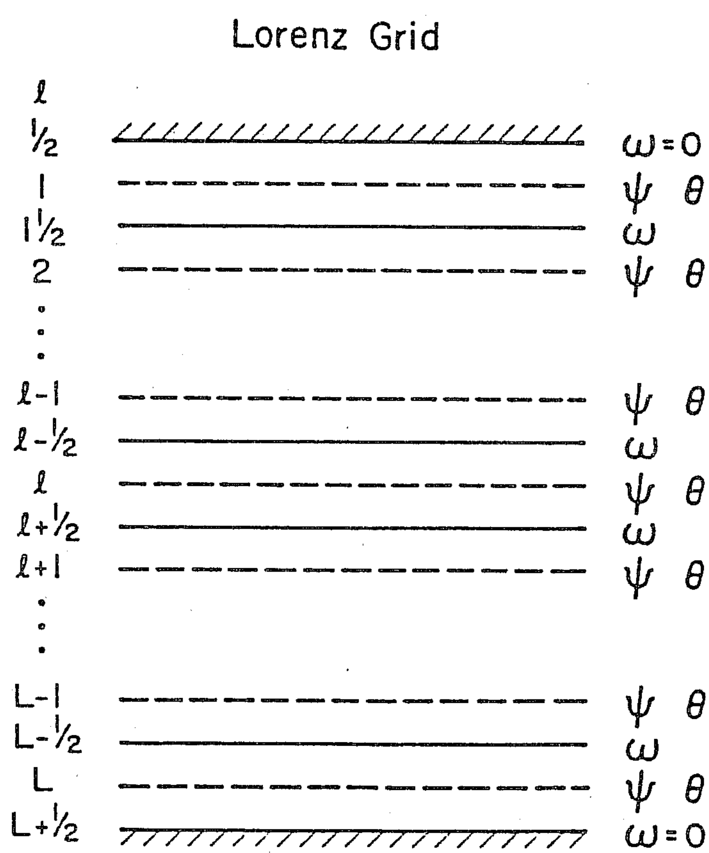

Fig. 3 The vertical grid used by Lorenz (1960).
See text for explanations.

In this grid, ψ, χ, ϕ and θ are defined for each layer, which is identified by an integer value of ℓ; while ω is carried at each level that separates the layers, which is identified by a half-integer value of ℓ. After rewritting the last term in (57) as $\partial(\omega\nabla\psi)/\partial p - (\partial\omega/\partial p)\nabla\psi$, all vertical derivatives with respect to p in (57), (59) and (60) can be replaced by vertical differences following

$$[\frac{\partial}{\partial p}(\ )]_\ell = \frac{(\ )_{\ell+\frac{1}{2}} - (\ )_{\ell-\frac{1}{2}}}{(\Delta p)_\ell} \quad . \tag{62}$$

For the results to be meaningful, however, ψ and θ at the half-integer levels with non-zero ω must be specified through some interpolations between the layers. Lorenz chose

$$\psi_{\ell+\frac{1}{2}} = \frac{1}{2}(\psi_\ell + \psi_{\ell+1}), \tag{63}$$

$$\theta_{\ell+\frac{1}{2}} = \frac{1}{2}(\theta_\ell + \theta_{\ell+1}), \tag{64}$$

and

$$\phi_\ell - \phi_{\ell+1} = c_p \theta_{\ell+\frac{1}{2}} [\ (p_{\ell+1}/p_o)^\kappa - (p_\ell/p_o)^\kappa\ ], \tag{65}$$

for $\ell = 1, 2, \ldots, L-1$, and

$$p_\ell = \frac{1}{2}(p_{\ell-\frac{1}{2}} + p_{\ell+\frac{1}{2}}). \tag{66}$$

The choices (63) and (65) were made to conserve total energy, while the choice (64) was made to conserve θ^2, integrated over the entire mass. Eq. (65) is a finite-difference analog of the hydrostatic equation written in the form

$$\frac{\partial\phi}{\partial(p/p_o)^\kappa} = -c_p\theta. \tag{67}$$

7. THE LORENZ VERTICAL DIFFERENCING APPLIED TO THE QUASI-GEOSTROPHIC FLOW

The merit of using the Lorenz grid in vertical differencing has been widely recognized, as far as a system of equations more general than the quasi-geostrophic system is concerned. In fact, most existing numerical weather prediction and general circulation models with the primitive equations are based on the Lorenz grid.

However, primary objectives of such models is still to predict or simulate large-scale disturbances which are nearly quasi-geostrophic in the extra-tropics, even though the quasi-geostrophic approximation is not explicitly used. An important question is then to find what the departure from the Charney-Phillips grid means to quasi-geostrophic flow. To seek an answer to this question, we shall examine the Lorenz vertical differencing applied to the system of quasi-geostrophic equations presented in Section 2.

To illustrate one of the problems with the Lorenz grid, let us consider a two-level (or two-layer) model as shown in Fig. 4.

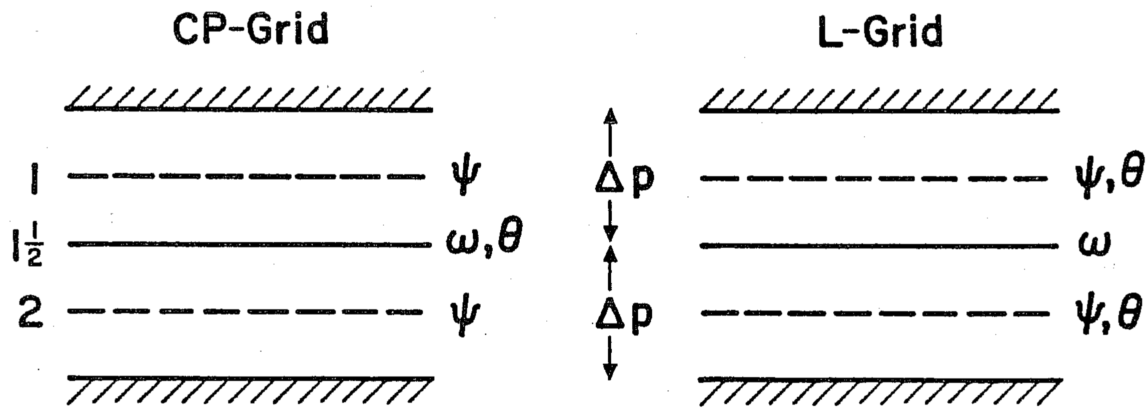

Fig. 4 Two-level models based on the Charney-Phillips grid and the Lorenz grid

The thermodynamic equation applied to level $1\frac{1}{2}$ of the Charney-Phillips grid is

$$\left(\frac{\partial}{\partial t} + \mathbf{v}_{1\frac{1}{2}} \cdot \nabla \right) \theta_{1\frac{1}{2}} + \omega \frac{d\bar{\theta}}{dp} = 0 \tag{68}$$

with $\mathbf{v}_{1\frac{1}{2}}$ obtained by using geostrophic $\mathbf{v}_1$ and $\mathbf{v}_2$ in (31). Here the subscripts $1\frac{1}{2}$ for ω and $d\bar{\theta}/dp$ have been omitted. Hereafter we shall use the definition

$$\frac{d\bar{\theta}}{dp} \equiv \frac{1}{\Delta p} \left(\bar{\theta}_2 - \bar{\theta}_1 \right). \tag{69}$$

The thermodynamic equations applied to levels 1 and 2 of the Lorenz grid are

$$\frac{\partial}{\partial t}\theta_1 + \nabla \cdot (\mathbf{v}_1 \theta_1) + \frac{\omega\ \theta_{1\frac{1}{2}}}{\Delta p} = 0 \tag{70}$$

$$\frac{\partial}{\partial t}\theta_2 + \nabla \cdot (\mathbf{v}_2 \theta_2) - \frac{\omega\ \theta_{1\frac{1}{2}}}{\Delta p} = 0. \tag{71}$$

Here $\mathbf{v}_1$ and $\mathbf{v}_2$ are non-geostrophic. Using the continuity equation

$$\nabla \cdot \mathbf{v}_1 + \frac{\omega}{\Delta p} = 0 \tag{72}$$

$$\nabla \cdot \mathbf{v}_2 - \frac{\omega}{\Delta p} = 0, \tag{73}$$

(70) and (71) may be rewritten as

$$\frac{\partial}{\partial t}\theta_1 + \mathbf{v}_1 \cdot \nabla \theta_1 + \frac{\omega}{\Delta p}(\theta_{1\frac{1}{2}} - \theta_1) = 0$$

$$\frac{\partial}{\partial t}\theta_2 + \mathbf{v}_2 \cdot \nabla \theta_2 + \frac{\omega}{\Delta p}(\theta_2 - \theta_{1\frac{1}{2}}) = 0. \tag{75}$$

Replacing v_1 and v_2 now by the corresponding geostrophic velocity, using (64), replacing $\theta_2 - \theta_1$ coupled with ω by $\bar{\theta}_2 - \bar{\theta}_1$, and using the definition (69), we obtain

$$\frac{\partial}{\partial t}\theta_1 + \mathbf{v}_1 \cdot \nabla\theta_1 + \frac{\omega}{2}\frac{d\bar{\theta}}{dp} = 0, \tag{76}$$

$$\frac{\partial}{\partial t}\theta_2 + \mathbf{v}_2 \cdot \nabla\theta_2 + \frac{\omega}{2}\frac{d\bar{\theta}}{dp} = 0. \tag{77}$$

The factor $\frac{1}{2}$ on ω appears since thermodynamic equation is applied to the dashed line levels in Fig. 4. If we neglect $(\mathbf{v}_1 - \mathbf{v}_2)\cdot\nabla(\theta_1 - \theta_2)$, (76), (77) and (64) give

$$(\frac{\partial}{\partial t} + \mathbf{v}_{1\frac{1}{2}}\cdot\nabla)\theta_{1\frac{1}{2}} + \omega\,\frac{1}{2}\frac{d\bar{\theta}}{dp} = 0. \tag{78}$$

Note that $\theta_{1\frac{1}{2}}$ is the potential temperature which is related to the thickness between levels 1 and 2 (see (65)), and therefore to $\psi_1 - \psi_2$. By comparing (78) with (68), we see that the effective static stability in the two-level model with the Lorenz grid is one-half of that with the Charney-Phillips grid.

The second problem with the Lorenz grid is that, in an L-layer model, there are L degrees of freedom in θ, while there are only L-1 degrees of freedom in the vertical differences of ψ. This means that there is an extra degree of freedom in θ that cannot satisfy a thermal wind relationship.

The third problem is that the governing equation cannot be written in a compact form such as (32) and a discrete analog of the potential vorticity cannot be easily defined. Let us define a " (pseudo-) potential vorticity equation " by an equation that does not involve ω, obtained by a linear combination of the vorticity and thermodynamic equations. In an L-layer model, there are L vorticity equations and L thermodynamic equations. If we eliminate L-1 non-zero ω from these 2L equations, we obtain L+1 " potential vorticity equations ", while there are only L potential vorticity equations with the Charney-Phillips grid.

The " potential vorticity equation " in the above sense with the Lorenz grid may be written as

$$\frac{D_1}{Dt}(\zeta_1 + f) + \frac{f_o}{\Delta p}\frac{1}{(\bar{\theta}_{1\frac{1}{2}} - \bar{\theta}_1)/\Delta p}\frac{D_1\theta_1}{Dt} = 0\,, \tag{79}$$

$$\frac{\bar{\theta}_{2\frac{1}{2}} - \bar{\theta}_2}{\bar{\theta}_{2\frac{1}{2}} - \bar{\theta}_{1\frac{1}{2}}}\frac{D_2}{Dt}(\zeta_2 + f) + \frac{f_o}{\Delta p}\left[\frac{1}{(\bar{\theta}_{2\frac{1}{2}} - \bar{\theta}_{1\frac{1}{2}})/\Delta p}\frac{D_2\theta_2}{Dt} - \frac{1}{(\bar{\theta}_{1\frac{1}{2}} - \bar{\theta}_1)/\Delta p}\frac{D_1\theta_1}{Dt}\right] = 0, \tag{80}$$

$$\frac{\bar{\theta}_{\ell+1\frac{1}{2}} - \bar{\theta}_{\ell+1}}{\bar{\theta}_{\ell+1\frac{1}{2}} - \bar{\theta}_{\ell+\frac{1}{2}}} \frac{D_{\ell+1}}{Dt}(\zeta_{\ell+1} + f) + \frac{\bar{\theta}_{\ell} - \bar{\theta}_{\ell-\frac{1}{2}}}{\bar{\theta}_{\ell+\frac{1}{2}} - \bar{\theta}_{\ell-\frac{1}{2}}} \frac{D_{\ell}}{Dt}(\zeta_{\ell} + f)$$

$$+ \frac{f_o}{\Delta p}\left[\frac{1}{(\bar{\theta}_{\ell+1\frac{1}{2}} - \bar{\theta}_{\ell+\frac{1}{2}})/\Delta p} \frac{D_{\ell+1}\theta_{\ell+1}}{Dt} - \frac{1}{(\bar{\theta}_{\ell+\frac{1}{2}} - \bar{\theta}_{\ell-\frac{1}{2}})/\Delta p} \frac{D_{\ell}\theta_{\ell}}{Dt}\right] = 0$$

$$\text{for } \ell = 2, 3, \ldots, L-2, \tag{81}$$

$$\frac{\bar{\theta}_{L-1} - \bar{\theta}_{L-1\frac{1}{2}}}{\bar{\theta}_{L-\frac{1}{2}} - \bar{\theta}_{L-1\frac{1}{2}}} \frac{D_{L-1}}{Dt}(\zeta_{L-1} + f)$$

$$+ \frac{f_o}{\Delta p}\left[\frac{1}{(\bar{\theta}_{L} - \bar{\theta}_{L-\frac{1}{2}})/\Delta p} \frac{D_L\theta_L}{Dt} - \frac{1}{(\bar{\theta}_{L-\frac{1}{2}} - \bar{\theta}_{L-1\frac{1}{2}})/\Delta p} \frac{D_{L-1}\theta_{L-1}}{Dt}\right] = 0, \tag{82}$$

$$\frac{D_L}{Dt}(\zeta_L + f) - \frac{f_o}{\Delta p} \frac{1}{(\bar{\theta}_L - \bar{\theta}_{L-\frac{1}{2}})/\Delta p} \frac{D_L\theta_L}{Dt} = 0. \tag{83}$$

Here

$$\frac{D_\ell}{Dt} \equiv \left(\frac{\partial}{\partial t} + \mathbf{v}_\ell \cdot \nabla \right) \tag{84}$$

and, for simplicity, Δp has been assumed constant.

To interpret the above "potential vorticity equations", it should be noted that q in the continuous case defined by (10) with $S \equiv -(\alpha/\theta)d\bar{\theta}/dp$ may be rewritten as

$$q = \zeta + f - f_o \frac{\partial}{\partial p}\left(\frac{\theta}{\sigma}\right), \tag{85}$$

where $\sigma \equiv -d\bar{\theta}/dp$. Let us now consider (79) through (83) for a sufficiently small Δp (i.e., a sufficiently large L). Then,

$$\frac{D_{\ell+1}}{Dt} \doteq \frac{D_\ell}{Dt} \tag{86}$$

may be used <u>within</u> each of the equations as a crude approximation. In addition, from (64) we obtain

$$\frac{\bar{\theta}_{\ell+\frac{1}{2}} - \bar{\theta}_{\ell}}{\Delta p} = \frac{1}{2} \frac{\bar{\theta}_{\ell+1} - \bar{\theta}_{\ell}}{\Delta p}, \tag{87}$$

$$\frac{\bar{\theta}_{\ell} - \bar{\theta}_{\ell-\frac{1}{2}}}{\Delta p} = \frac{1}{2} \frac{\bar{\theta}_{\ell} - \bar{\theta}_{\ell-1}}{\Delta p} \tag{88}$$

and, therefore,

$$\frac{\bar{\theta}_{\ell+\frac{1}{2}} - \bar{\theta}_{\ell-\frac{1}{2}}}{\Delta p} = \frac{\bar{\theta}_{\ell+1} - \bar{\theta}_{\ell-1}}{2\Delta p} \tag{89}$$

In the following we use the notation

$$\sigma_{\ell+\frac{1}{2}} \equiv - \frac{\theta_{\ell+1} - \theta_{\ell}}{\Delta p} \quad . \tag{90}$$

Using (86) through (90) in (79) through (83), we can define approximate expressions for the potential vorticity with the Lorenz grid as follows:

$$q_1 = \zeta_1 + f - \frac{2f_o}{\Delta p} \frac{\theta_1}{\sigma_{1\frac{1}{2}}} , \tag{91}$$

$$q_{1\frac{1}{2}} = \frac{\sigma_{2\frac{1}{2}}}{\sigma_{2\frac{1}{2}} + \sigma_{1\frac{1}{2}}} (\zeta_2 + f) - \frac{2f_o}{\Delta p} [\frac{\theta_2}{\sigma_{2\frac{1}{2}} + \sigma_{1\frac{1}{2}}} - \frac{\theta_1}{\sigma_{1\frac{1}{2}}}] , \tag{92}$$

$$q_{\ell+\frac{1}{2}} = \frac{\sigma_{\ell+1\frac{1}{2}}}{\sigma_{\ell+1\frac{1}{2}} + \sigma_{\ell+\frac{1}{2}}} (\zeta_{\ell+1} + f) + \frac{\sigma_{\ell-\frac{1}{2}}}{\sigma_{\ell+\frac{1}{2}} + \sigma_{\ell-\frac{1}{2}}} (\zeta_\ell + f)$$

$$- \frac{2f_o}{\Delta p} [\frac{\theta_{\ell+1}}{\sigma_{\ell+1\frac{1}{2}} + \sigma_{\ell+\frac{1}{2}}} - \frac{\theta_\ell}{\sigma_{\ell+\frac{1}{2}} + \sigma_{\ell-\frac{1}{2}}}] \quad \text{for } \ell = 2,3,\cdots,L-2, \tag{93}$$

$$q_{L-\frac{1}{2}} = \frac{\sigma_{L-1\frac{1}{2}}}{\sigma_{L-\frac{1}{2}} + \sigma_{L-1\frac{1}{2}}} (\zeta_{L-1} + f) - \frac{2f_o}{\Delta p} [\frac{\theta_L}{\sigma_{L-\frac{1}{2}}} - \frac{\theta_{L-1}}{\sigma_{L-\frac{1}{2}} + \sigma_{L-1\frac{1}{2}}}] , \tag{94}$$

$$q_L = (\zeta_L + f) + \frac{2f_o}{\Delta p} \frac{\theta_L}{\sigma_{L-\frac{1}{2}}} \quad . \tag{95}$$

It should be noted that in the limit as $\Delta p \to 0$ (95) involves the delta function, as (36) for the Charney-Phillips grid does. The same is true for (91). A feature unique to the Lorenz grid is in (92) and (94). Eq. (94), for example, also involves the delta function in the limit as $\Delta p \to 0$, but with a coefficient whose sign is opposite to that of (95). A similar situation exists between (91) and (92).

8. BAROCLINIC INSTABILITY WITH THE CHARNEY-PHILLIPS AND LORENZ GRIDS

The argument given in the last section indicates that there can be significant differences between the solutions of the two types of discrete models, one based on the Charney-Phillips grid and the other based on the Lorenz grid, whenever the lower (or upper) boundary conditions play an important role. In this section we compare the two types of discrete models in view of baroclinic instability of horizontally uniform zonal flow with respect to a small-amplitude y-independent wave disturbance. An f-plane and a β-plane, both centered at 45°N, and p_T = 100 mb and p_S = 1000 mb are used.

When the modified potential vorticity $\tilde{q}$ defined by (37) is used, one of the necessary conditions for baroclinic instability (Charney and Stern, 1962) applied to the above problem is that $\partial\tilde{Q}/\partial y$ must change sign in vertical. Here $\tilde{Q}$ is $\tilde{q}$ for the basic state;

$$\frac{\partial\tilde{Q}}{\partial y} = \beta - f_o^2 \frac{d}{dp}\left(\frac{1}{S}\frac{dU}{dp}\right) + \frac{f_o^2}{S}\left(\frac{dU}{dp}\right)_{p=p_S} \delta(p_S - p) - \frac{f_o^2}{S}\left(\frac{dU}{dp}\right)_{p=p_S} \delta(p - p_T); \qquad (96)$$

and U(p) is the basic zonal flow (eastward positive).

For simplicity, we shall only consider the case where S = constant ($= 2\times10^{-2}m^2sec^{-2}mb^{-2}$) and dU/dp = constant < 0 (i.e., a profile linear in p with westerly shear). Then the second term on the right hand side of (96) vanishes.

(a) $\beta = 0$

Let us first consider the case of f-plane, for which $\beta = 0$. This case is equivalent to the Eady model (Eady, 1949), for which the analytic solution is known. In this model $\partial\tilde{Q}/\partial y$ changes sign due to the existence of the two boundary terms in (96).

Fig. 5 shows the growth rates as functions of wavelength and vertical shear, with the Charney-Phillips grid (the left panels) and the Lorenz grid (the right panels). the upper, middle and lower panels are the results obtained from the 2-level, 6-level and 18-level models, respectively. (With the Lorenz grid, the vertical differencing of Arakawa and Suarez (1983) was used instead of the original Lorenz vertical differencing.)

As we can see from the figure, the cutoff wavelength of the 2-level model is shorter with the Lorenz grid than that with the Charney-Phillips grid. This is anticipated since the effective static stability with the Lorenz grid is roughly one half of that with the Charney-Phillips grid, as pointed out in Section 7.

The most remarkable feature in Fig. 5 is the rapid growth of short waves in multi-level models with the Lorenz grid. This is obviously spurious since it contradicts the analytic solution of the Eady model. The maximum of this spurious growth rate shifts toward shorter wavelengths as the vertical resolution increases. This can be more clearly seen in Fig. 6, in which the growth rates for $|dU/dp| = 5$ m sec^{-1}/100 mb are shown as functions of wavelength and the number of levels. Note that the growth rate with the Charney-Phillips grid rapidly converges as the number of levels increases, while that with the Lorenz grid converges very slowly. Even with the 30-level model the spurious growth rate is still very large though it appears for very short wavelengths.

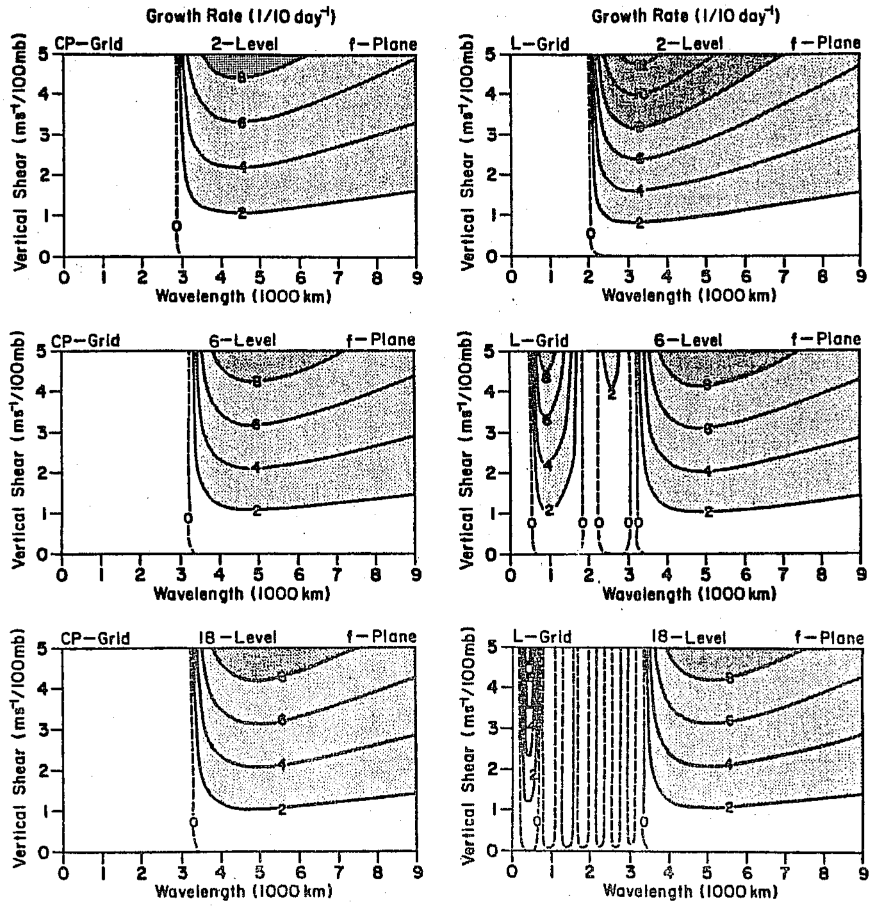

Fig. 5 Growth rates in $10^{-1}day^{-1}$ as functions of wavelength and vertical shear obtained from the 2-level, 6-level and 18 level models with the Charney-Phillips and Lorenz grids on an f-plane.

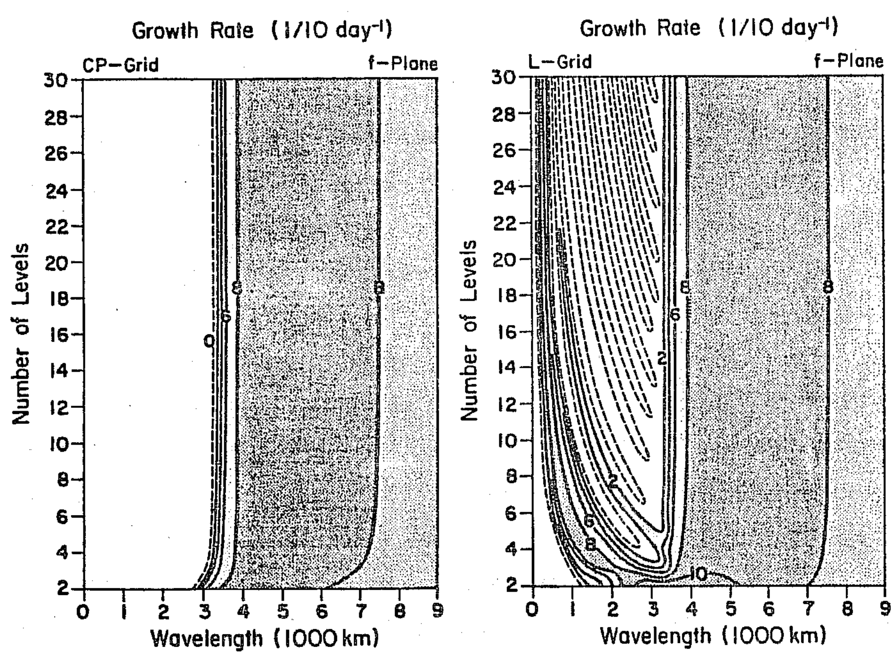

Fig. 6 Growth rates in $10^{-1}day^{-1}$ for $|dU/dp| = 5$ m sec^{-1} $(100 \text{ mb})^{-1}$ as functions of wavelength and the number of levels with the Charney-Phillips and Lorenz grids on an f-plane.

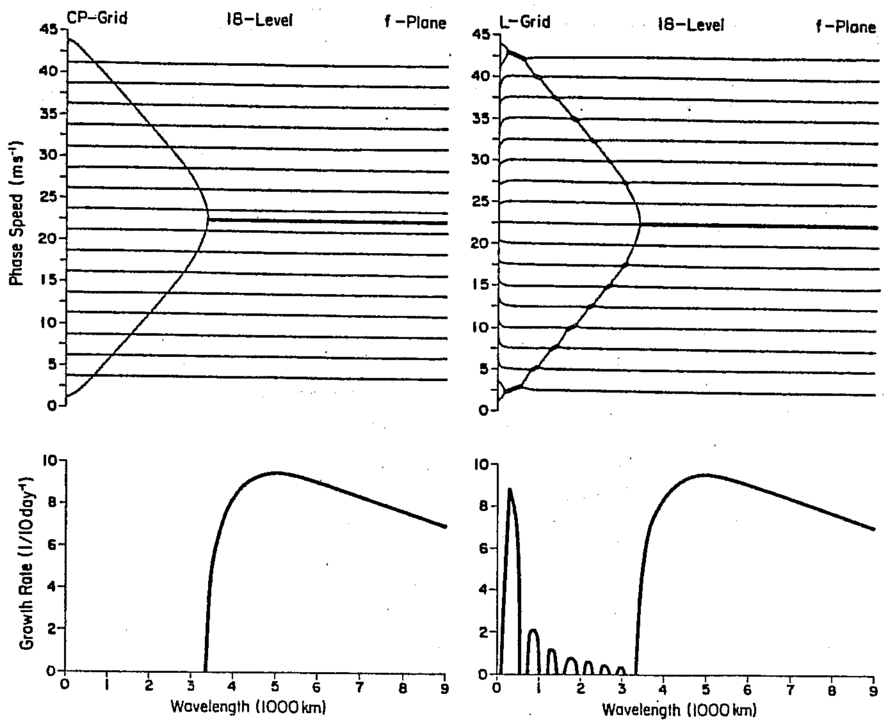

Fig. 7 Phase speeds in m sec^{-1} and growth rates in 10^{-1} day^{-1} as functions of wavelength for $|dU/dp| = 5$ m sec^{-1} $(100 \text{ mb})^{-1}$ obtained from the 18-level model with the Charney-Phillips and Lorenz grids on an f-plane.

The upper panels of Fig. 7 show the phase speed (the real part of the complex phase speed c), relative to U of the bottom boundary, of various modes in the 18-level models for the same $|dU/dp|$. On the heavy parts of the lines c is a pair of complex conjugates; while on the thin parts of the lines c is real. Parallel or nearly parallel thin lines correspond to neutral singular modes in the continuous case. The steering levels of these modes with the Charney-Phillips grid are approximately at $\ell = 2, 3, \ldots, L-1$, while those with the Lorenz grid are approximately at $\ell = 1\frac{1}{2}, 2\frac{1}{2}, \ldots, L-\frac{1}{2}$. Note that these are the levels where q is defined (see (34), (92), (93) and (94)). The lower panels of Fig. 7 show the growth rates of amplifying modes as functions of wavelength. Fig. 8 shows the structure of amplifying modes with the Lorenz grid for two selected wavelengths. The upper panel is for a spuriously amplifying mode, while the lower panel is for the amplifying Eady mode. Fig. 9 gives an example of the structure of neutral modes.

(b) $\beta \neq 0$

This case is equivalent to the Green model with the Boussinesq approximation. As Green (1960) showed, the inclusion of β eliminates the short-wave cutoff of the Eady model. The results for this case are shown in Figs. 10, 11 and 12, which correspond to Figs. 5, 6 and 7 for the f-plane case, respectively.

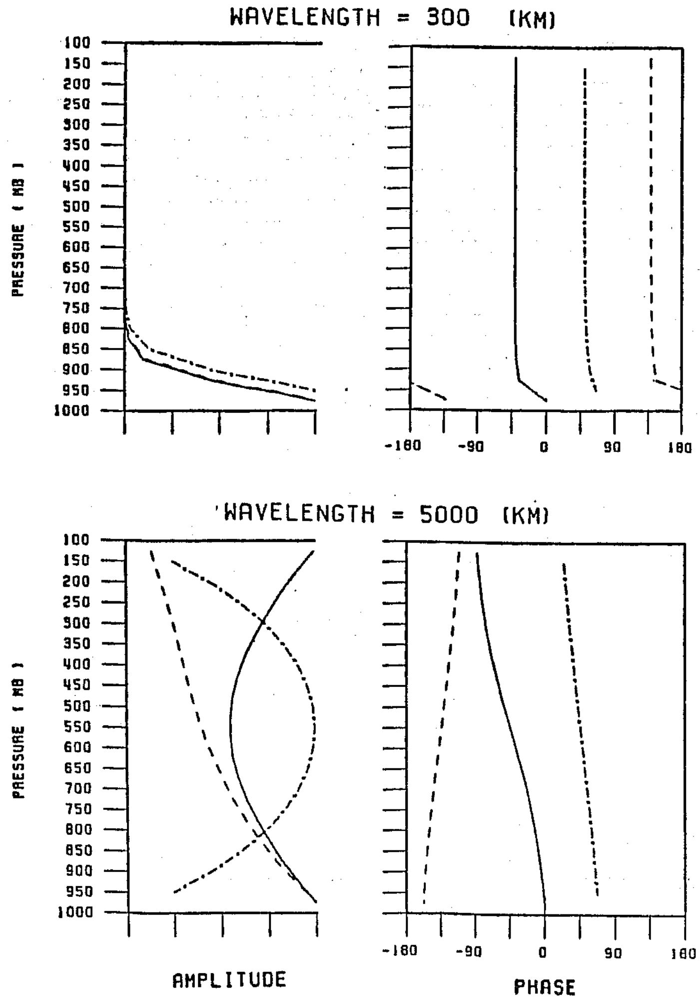

Fig. 8 The amplitude and phase of amplifying modes shown in the right panel of Fig. 7. The upper panel: a mode with the lowest steering level at the wavelength of 300 km. The lower panel: the Eady mode at the wavelength of 5000 km. The solid, dashed and chain lines are for the normalized streamfunction, temperature, and vertical p-velocity perturbations, respectively.

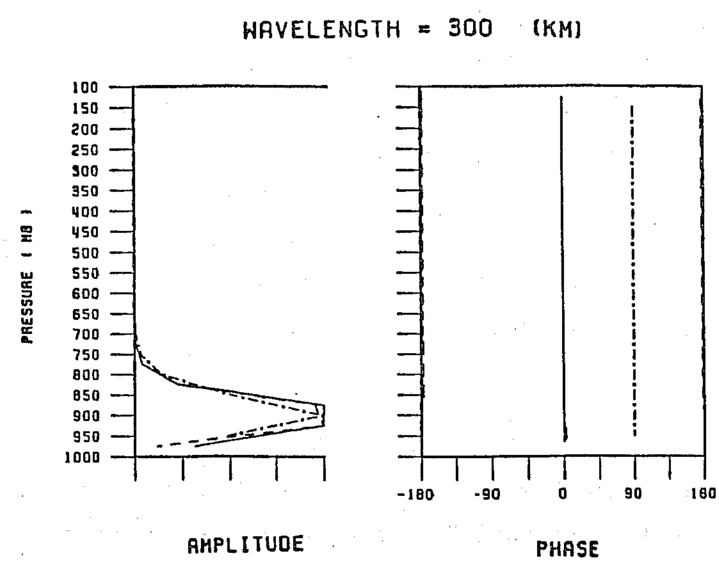

Fig. 9 The same as Fig. 8 but for a neutral mode with the lowest steering level at the wavelength of 300 km.

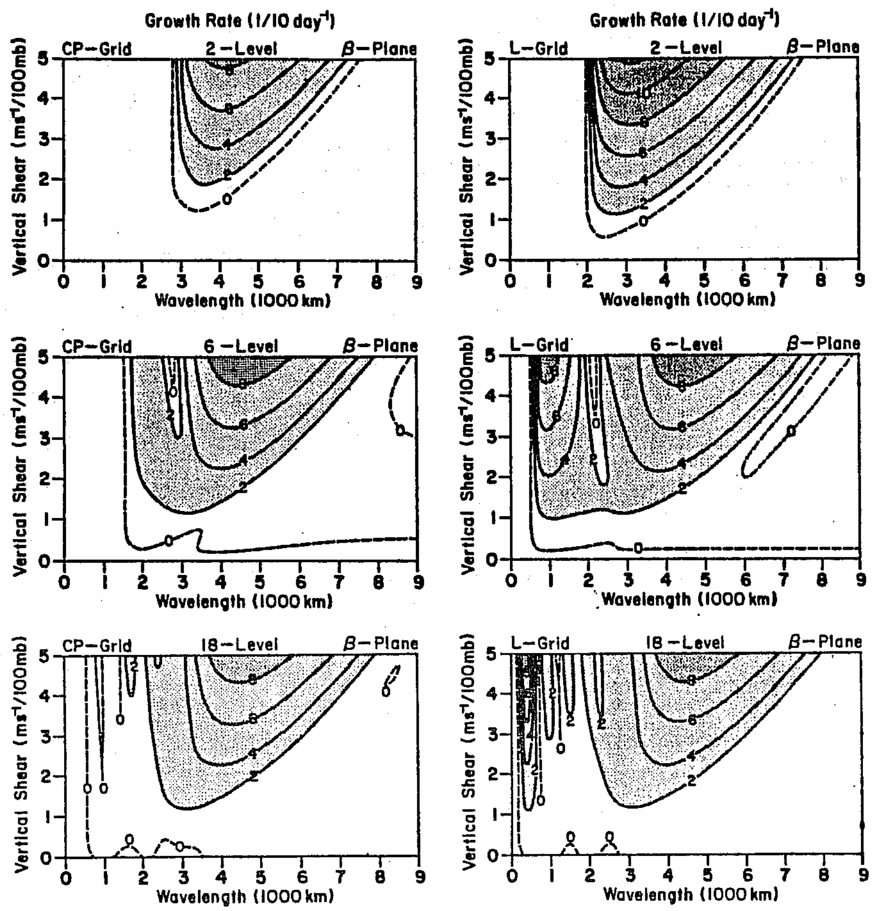

Fig. 10 The same as Fig. 5 but for a β-plane.

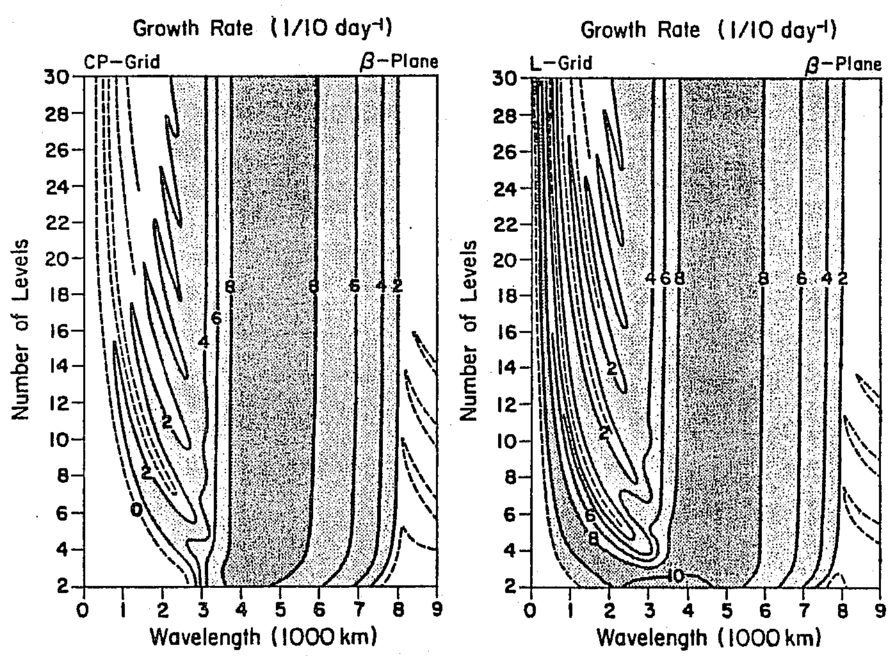

Fig. 11 The same as Fig. 6 but for a β-plane.

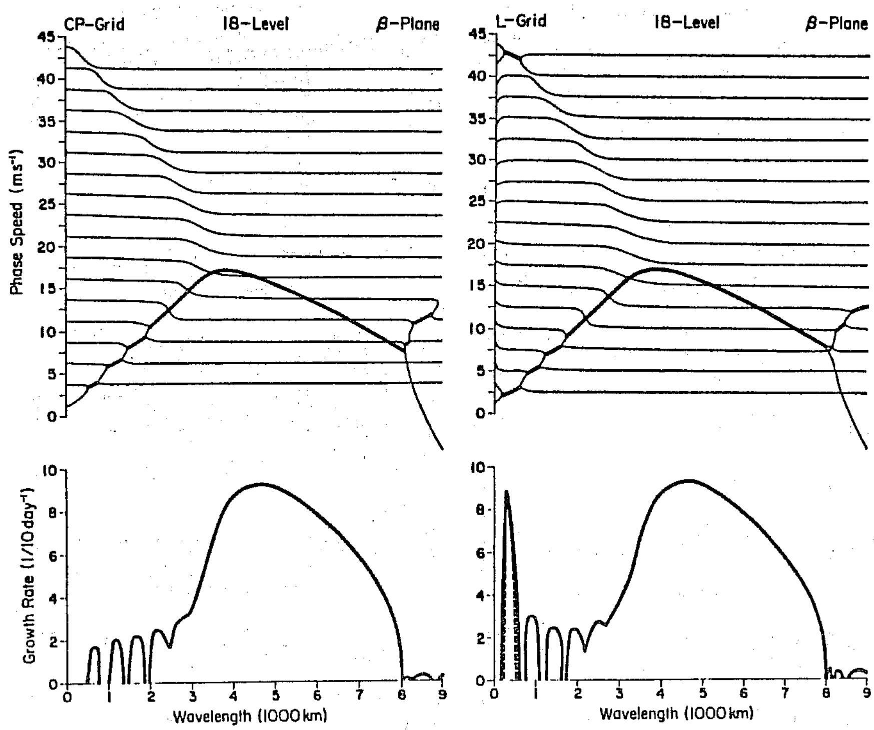

Fig. 12 The same as Fig. 7 but for a β-plane. The dashed line shows the growth rate of the amplifying mode with a steering level near the upper boundary.

Rapid growth of short waves in multi-level models with the Lorenz grid is again apparent in these figures. The shortest-wave peak must be highly spurious as in the f-plane case. Minor peaks, which also appear in multi-level models with the Charney-Phillips grid, are probably associated with critical layer instability with non-zero $\partial Q/\partial y$ (Bretherton, 1966). The growth rate spectrum is discrete, however, because there are only discrete critical levels.

A similar analysis has been performed for a more realistic vertical distribution of the static stability parameter S. The result shows that the spurious growth of short waves trapped near the bottom boundary is even larger. In a model that includes condensation processes, the spurious growth can be even more drastic. Since the supply of moisture available for condensation is more or less limited, the spurious growth of small-scale motions in a nonlinear model will decrease the amount of moisture available for condensation due to synoptic-scale waves and thereby produce errors in their dynamics.

We hypothesize that this spurious growth is a consequence of the existence of the delta function in (92) and (94) in the limit as $\Delta p \to 0$. To verify this hypothesis and to obtain a guide for overcoming this problem, we have recalculated the growth rates with the additional term

$$- k \left(\theta_1 - \frac{\sigma_{1\frac{1}{2}}}{\sigma_{2\frac{1}{2}} + \sigma_{1\frac{1}{2}}} \theta_2 \right) \quad (97)$$

in the right hand side of the $\partial\theta_1/\partial t$ equation and the term

$$- k \left(\theta_L - \frac{\sigma_{L-\frac{1}{2}}}{\sigma_{L-\frac{1}{2}} + \sigma_{L-1\frac{1}{2}}} \theta_{L-1} \right) \quad (98)$$

in the right hand side of the $\partial\theta_L/\partial t$ equation. The addition of these terms prevents the quantities in the brackets in (92) and (94) from being very large. We have found that the results are insensitive to even the order of magnitude of the coefficient k, if $k \gtrsim 10^{-3}$ $\sec^{-1}$. The dotted lines in Fig. 13 show the modified growth rate. Note that the shortest wavelength peak has been practically eliminated, while the growth rates for longer wavelengths remain approximately the same.

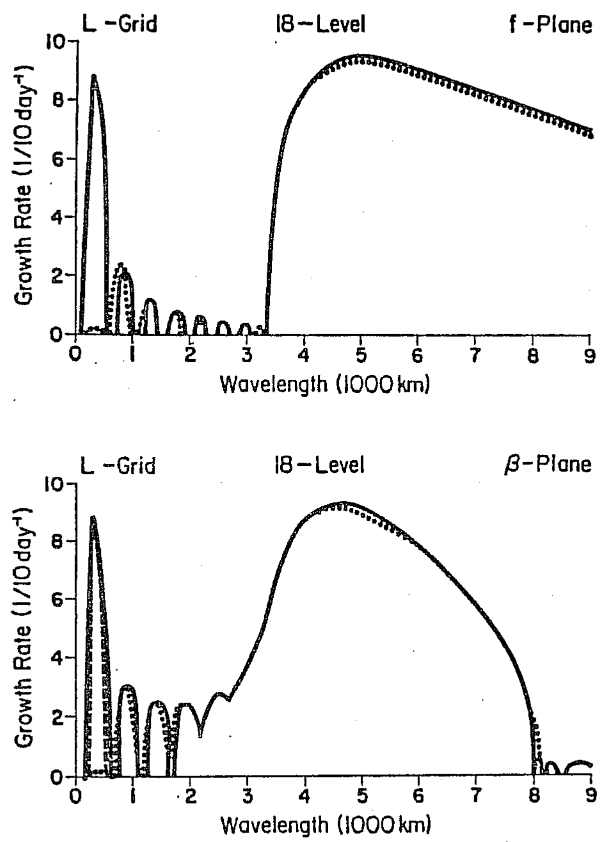

Fig. 13 The same as the bottom right panels of Fig. 7 and 12. The dotted lines show the modified growth rate with the terms (97) and (98).

9. SUMMARY AND CONCLUSIONS

The vertical differencing of Charney and Phillips (1953) for the quasi-geostrophic system of equations based on the grid shown by Fig. 1 is very straight-forward, especially in that there exists an analog of the quasi-geostrophic (pseudo-) potential vorticity.

On the other hand, as Lorenz (1960) showed, the grid shown by Fig. 3 is more convenient to maintain conservation of energy and enthalpy for more general flow in a discrete system. One of the disadvantages of this grid is the lack of a clean analog of the quasi-geostrophic (pseudo-) potential vorticity, a consequence of which is the growth of sub-synoptic scale waves due to spurious baroclinic instability. It seems, however, this difficulty can be practically eliminated by modifying the (potential) temperature prediction equation for the bottom and top layers.

References

Arakawa, A., 1962: Non-geostrophic effects in the baroclinic prognostic equations. Proc. Intern. Symp. Numerical Weather Prediction, Tokyo, 161-175.

Arakawa, A., and M.J. Suarez, 1983: Vertical differencing of the primitive equations in sigma coordinates. J. Atmos. Sci., 111, 34-45.

Bretherton, F.P., 1966: Critical layer instability in baroclinic flows. Quart. J. Roy. Meteor. Soc., 92, 325-334.

Charney, J.G. and N.A. Phillips, 1953: Numerical integration of the quasi-geostrophic equations for barotropic and simple baroclinic flows. J. Meteor., 10, 71-99.

Charney, J.G., 1955: The use of primitive equations of motion in numerical prediction. Tellus, 7, 22-26.

Charney, J.G., M. Stern, 1962: On the stability of internal baroclinic jets in a rotating atmosphere. J. Atmos. Sci., 19, 159-172.

Charney, J.G., 1971: Geostrophic turbulence. J. Atmos. Sci., 28, 1087-1095.

Eady, E.T., 1949: Long waves and cyclone waves. Tellus, 1, 33-52.

Green, J.S.A., 1960: A problem in baroclinic stability. Quart. J. Roy. Meteor. Soc., 86, 237-251.

Haltiner, G.J., and R.T. Williams, 1980: Numerical prediction and dynamic meteorology, John Wiley & Sons, 477 pp.

Holton, J.R., 1979: An introduction to dynamic meteorology. Academic Press, 391 pp.

Lorenz, E.N, 1955: Available potential energy and the maintenance of the general circulation. Tellus, 7, 157-167.

Lorenz, E.N., 1960: Energy and numerical weather prediction. Tellus, 12, 364-373.